



TITLE:

Radiative B meson decays into K pi gamma and K pi pi gamma final states

AUTHOR(S):

Nishida, S; Nakao, M; Abe, K; Abe, K; Abe, T; Ahn, BS; Aihara, H; ... Zhang, ZP; Zhilich, V; Zontar, D

CITATION:

Nishida, S ...[et al]. Radiative B meson decays into K pi gamma and K pi pi gamma final states. PHYSICAL REVIEW LETTERS 2002, 89(23): 231801.

ISSUE DATE:

2002-12-02

URL:

<http://hdl.handle.net/2433/49942>

RIGHT:

Copyright 2002 American Physical Society

Radiative B Meson Decays into $K\pi\gamma$ and $K\pi\pi\gamma$ Final States

S. Nishida,¹⁸ M. Nakao,¹⁰ K. Abe,¹⁰ K. Abe,⁴³ T. Abe,⁴⁴ Byoung Sup Ahn,¹⁷ H. Aihara,⁴⁵ M. Akatsu,²⁴ Y. Asano,⁴⁹ T. Aushev,¹⁴ A. M. Bakich,⁴⁰ Y. Ban,³⁵ E. Banas,²⁹ W. Bartel,⁶ A. Bay,²⁰ I. Bedny,² A. Bondar,² A. Bozek,²⁹ M. Bračko,^{22,15} J. Brodzicka,²⁹ T. E. Browder,⁹ B. C. K. Casey,⁹ P. Chang,²⁸ Y. Chao,²⁸ B. G. Cheon,³⁹ R. Chistov,¹⁴ S.-K. Choi,⁸ Y. Choi,³⁹ M. Danilov,¹⁴ L. Y. Dong,¹² A. Drutskoy,¹⁴ S. Eidelman,² V. Eiges,¹⁴ Y. Enari,²⁴ C. Fukunaga,⁴⁷ N. Gabyshev,¹⁰ T. Gershon,¹⁰ A. Gordon,²³ K. Gotow,⁵¹ R. Guo,²⁶ J. Haba,¹⁰ T. Hara,³³ H. Hayashii,²⁵ M. Hazumi,¹⁰ E. M. Heenan,²³ I. Higuchi,⁴⁴ T. Higuchi,⁴⁵ T. Hojo,³³ T. Hokuue,²⁴ Y. Hoshi,⁴³ S. R. Hou,²⁸ W.-S. Hou,²⁸ S.-C. Hsu,²⁸ H.-C. Huang,²⁸ T. Igaki,²⁴ T. Iijima,²⁴ K. Inami,²⁴ A. Ishikawa,²⁴ H. Ishino,⁴⁶ R. Itoh,¹⁰ M. Iwamoto,³ H. Iwasaki,¹⁰ Y. Iwasaki,¹⁰ P. Jalocho,²⁹ H. K. Jang,³⁸ J. H. Kang,⁵³ P. Kapusta,²⁹ S. U. Kataoka,²⁵ N. Katayama,¹⁰ H. Kawai,³ Y. Kawakami,²⁴ N. Kawamura,¹ T. Kawasaki,³¹ H. Kichimi,¹⁰ D. W. Kim,³⁹ Heejong Kim,⁵³ H. J. Kim,⁵³ H. O. Kim,³⁹ Hyunwoo Kim,¹⁷ T. H. Kim,⁵³ K. Kinoshita,⁵ P. Križan,^{21,15} P. Krokovny,² R. Kulasiri,⁵ S. Kumar,³⁴ Y.-J. Kwon,⁵³ J. S. Lange,^{7,36} G. Leder,¹³ S. H. Lee,³⁸ J. Li,³⁷ R.-S. Lu,²⁸ J. MacNaughton,¹³ G. Majumder,⁴¹ F. Mandl,¹³ S. Matsumoto,⁴ T. Matsumoto,^{24,47} Y. Mikami,⁴⁴ W. Mitaroff,¹³ K. Miyabayashi,²⁵ H. Miyake,³³ H. Miyata,³¹ G. R. Moloney,²³ S. Mori,⁴⁹ T. Nagamine,⁴⁴ Y. Nagasaka,¹¹ T. Nakadaira,⁴⁵ E. Nakano,³² J. W. Nam,³⁹ Z. Natkaniec,²⁹ K. Neichi,⁴³ O. Nitoh,⁴⁸ S. Noguchi,²⁵ T. Nozaki,¹⁰ S. Ogawa,⁴² F. Ohno,⁴⁶ T. Ohshima,²⁴ T. Okabe,²⁴ S. Okuno,¹⁶ S. L. Olsen,⁹ W. Ostrowicz,²⁹ H. Ozaki,¹⁰ P. Pakhlov,¹⁴ H. Palka,²⁹ C. W. Park,¹⁷ H. Park,¹⁹ K. S. Park,³⁹ L. S. Peak,⁴⁰ J.-P. Perroud,²⁰ M. Peters,⁹ L. E. Pilonen,⁵¹ M. Rozanska,²⁹ K. Rybicki,²⁹ H. Sagawa,¹⁰ S. Saitoh,¹⁰ Y. Sakai,¹⁰ H. Sakamoto,¹⁸ M. Satapathy,⁵⁰ A. Satpathy,^{10,5} O. Schneider,²⁰ S. Schrenk,⁵ C. Schwanda,^{10,13} S. Semenov,¹⁴ K. Senyo,²⁴ R. Seuster,⁹ M. E. Sevier,²³ H. Shibuya,⁴² B. Schwartz,² V. Sidorov,² J. B. Singh,³⁴ S. Stanič,^{49,*} A. Sugi,²⁴ A. Sugiyama,²⁴ K. Sumisawa,¹⁰ T. Sumiyoshi,^{10,47} K. Suzuki,¹⁰ S. Suzuki,⁵² T. Takahashi,³² F. Takasaki,¹⁰ K. Tamai,¹⁰ N. Tamura,³¹ M. Tanaka,¹⁰ G. N. Taylor,²³ Y. Teramoto,³² S. Tokuda,²⁴ M. Tomoto,¹⁰ T. Tomura,⁴⁵ S. N. Tovey,²³ K. Trabelsi,⁹ T. Tsuboyama,¹⁰ T. Tsukamoto,¹⁰ S. Uehara,¹⁰ K. Ueno,²⁸ S. Uno,¹⁰ Y. Ushiroda,¹⁰ G. Varner,⁹ K. E. Varvell,⁴⁰ C. C. Wang,²⁸ C. H. Wang,²⁷ J. G. Wang,⁵¹ M.-Z. Wang,²⁸ Y. Watanabe,⁴⁶ E. Won,³⁸ B. D. Yabsley,⁵¹ Y. Yamada,¹⁰ A. Yamaguchi,⁴⁴ H. Yamamoto,⁴⁴ Y. Yamashita,³⁰ M. Yamauchi,¹⁰ Y. Yuan,¹² Y. Yusa,⁴⁴ J. Zhang,⁴⁹ Z. P. Zhang,³⁷ V. Zhilich,² and D. Žontar⁴⁹

(Belle Collaboration)

¹Aomori University, Aomori

²Budker Institute of Nuclear Physics, Novosibirsk

³Chiba University, Chiba

⁴Chuo University, Tokyo

⁵University of Cincinnati, Cincinnati, Ohio

⁶Deutsches Elektronen-Synchrotron, Hamburg

⁷University of Frankfurt, Frankfurt

⁸Gyeongsang National University, Chinju

⁹University of Hawaii, Honolulu, Hawaii

¹⁰High Energy Accelerator Research Organization (KEK), Tsukuba

¹¹Hiroshima Institute of Technology, Hiroshima

¹²Institute of High Energy Physics, Chinese Academy of Sciences, Beijing

¹³Institute of High Energy Physics, Vienna

¹⁴Institute for Theoretical and Experimental Physics, Moscow

¹⁵J. Stefan Institute, Ljubljana

¹⁶Kanagawa University, Yokohama

¹⁷Korea University, Seoul

¹⁸Kyoto University, Kyoto

¹⁹Kyungpook National University, Taegu

²⁰Institut de Physique des Hautes Énergies, Université de Lausanne, Lausanne

²¹University of Ljubljana, Ljubljana

²²University of Maribor, Maribor

²³University of Melbourne, Victoria

²⁴Nagoya University, Nagoya

²⁵Nara Women's University, Nara

²⁶National Kaohsiung Normal University, Kaohsiung

- ²⁷National Lien-Ho Institute of Technology, Miao Li
²⁸National Taiwan University, Taipei
²⁹H. Niewodniczanski Institute of Nuclear Physics, Krakow
³⁰Nihon Dental College, Niigata
³¹Niigata University, Niigata
³²Osaka City University, Osaka
³³Osaka University, Osaka
³⁴Panjab University, Chandigarh
³⁵Peking University, Beijing
³⁶RIKEN BNL Research Center, Brookhaven, New York
³⁷University of Science and Technology of China, Hefei
³⁸Seoul National University, Seoul
³⁹Sungkyunkwan University, Suwon
⁴⁰University of Sydney, Sydney, New South Wales
⁴¹Tata Institute of Fundamental Research, Bombay
⁴²Toho University, Funabashi
⁴³Tohoku Gakuin University, Tagajo
⁴⁴Tohoku University, Sendai
⁴⁵University of Tokyo, Tokyo
⁴⁶Tokyo Institute of Technology, Tokyo
⁴⁷Tokyo Metropolitan University, Tokyo
⁴⁸Tokyo University of Agriculture and Technology, Tokyo
⁴⁹University of Tsukuba, Tsukuba
⁵⁰Utkal University, Bhubaneswer
⁵¹Virginia Polytechnic Institute and State University, Blacksburg, Virginia
⁵²Yokkaichi University, Yokkaichi
⁵³Yonsei University, Seoul

(Received 12 May 2002; revised manuscript received 6 September 2002; published 13 November 2002)

We report observations of radiative B meson decays into the $K^+ \pi^- \gamma$ and $K^+ \pi^- \pi^+ \gamma$ final states. In the $B^0 \rightarrow K^+ \pi^- \gamma$ channel, we present evidence for decays via an intermediate tensor meson state with a branching fraction of $\mathcal{B}(B^0 \rightarrow K_2^*(1430)^0 \gamma) = [1.3 \pm 0.5(\text{stat}) \pm 0.1(\text{syst})] \times 10^{-5}$. We measure the branching fraction $\mathcal{B}(B^+ \rightarrow K^+ \pi^- \pi^+ \gamma) = [2.4 \pm 0.5(\text{stat}) \pm 0.4(\text{syst})] \times 10^{-5}$, in which the $B^+ \rightarrow K^{*0} \pi^+ \gamma$ and $B^+ \rightarrow K^+ \rho^0 \gamma$ channels dominate. The analysis is based on a data set of 29.4 fb^{-1} recorded by the Belle experiment at the KEKB collider.

DOI: 10.1103/PhysRevLett.89.231801

PACS numbers: 13.20.He, 13.40.Hq, 14.40.Nd

Since the first measurement of the inclusive branching fraction for $B \rightarrow X_s \gamma$ by the CLEO Collaboration in 1995 [1], the flavor changing neutral current process $b \rightarrow s \gamma$ has been used as a sensitive probe to search for physics beyond the standard model (SM). In experiments at the $Y(4S)$, a pseudoreconstruction technique, in which the X_s state is reconstructed from one kaon and multiple pions, has been the most powerful tool to identify $b \rightarrow s \gamma$ events. In order to measure more precisely the inclusive rate, a detailed knowledge of the exclusive final states is required. In addition to the already established $B \rightarrow K^* \gamma$ decay [2], there are several known resonances that can contribute to the final state. CLEO has reported evidence for $B \rightarrow K_2^*(1430) \gamma$ [3]. Some theoretical predictions for the branching fractions of the exclusive decays can be found in Ref. [4]. Exclusive decays, such as $B \rightarrow K_1(1400) \gamma$, can also be used to measure the photon helicity, which may differ from the SM prediction in some new physics models [5].

In this Letter, we report on a search for resonant structures K_X above the K^* mass in radiative B meson decays. The analysis is based on a data sample of

29.4 fb^{-1} ($31.9 \times 10^6 B \bar{B}$ events) recorded by the Belle detector [6] at KEKB [7]. KEKB is an asymmetric energy $e^+ e^-$ collider (3.5 GeV on 8 GeV) operated at the $Y(4S)$ resonance. The Belle detector has a three-layer silicon vertex detector, 50-layer central drift chamber (CDC), an array of aerogel Cherenkov counters (ACC), time-of-flight (TOF) scintillation counters, and an electromagnetic calorimeter of CsI(Tl) crystals (ECL).

We select events that contain a high energy photon (γ) with an energy between 1.8 and 3.4 GeV in the $Y(4S)$ center-of-mass (CM) frame and within the acceptance of the barrel ECL ($33^\circ < \theta_\gamma < 128^\circ$). In order to reduce the background from $\pi^0, \eta \rightarrow \gamma \gamma$ decays, we combine the photon candidate with all other photon clusters in the event and reject the candidate if the invariant mass of any pair is within $18 \text{ MeV}/c^2$ ($32 \text{ MeV}/c^2$) of the nominal π^0 (η) mass (this condition is referred to as the π^0/η veto).

We search for K_X resonances decaying into two-body ($K^+ \pi^-$) and three-body ($K^+ \pi^- \pi^+$) final states [8] in the invariant mass (M_{K_X}) range up to $2.4 \text{ GeV}/c^2$. For the $K^+ \pi^-$ final state, the range $M_{K_X} < 1.2 \text{ GeV}/c^2$ is

excluded to remove K^* contributions. Charged tracks are required to have CM momenta greater than 200 MeV/ c , and to have impact parameters within ± 5 cm of the interaction point along the positron beam axis and within 0.5 cm in the transverse plane. To identify kaon and pion candidates, we use a likelihood ratio that is calculated by combining information from the ACC, TOF, and dE/dx (CDC) systems. We apply a tight selection with an efficiency (pion misidentification rate) of 83% (8%) for charged kaon candidates and a loose selection with an efficiency (kaon misidentification rate) of 97% (28%) for charged pion candidates.

We reconstruct B meson candidates from a photon and a K_X system by forming two independent kinematic variables: the beam constrained mass $M_{bc} \equiv \sqrt{(E_{beam}^*/c^2)^2 - (|\vec{p}_{K_X}^* + \vec{p}_\gamma^*|/c)^2}$ and $\Delta E \equiv E_{K_X}^* + E_\gamma^* - E_{beam}^*$, where E_{beam}^* is the beam energy, and \vec{p}_γ^* , E_γ^* , $\vec{p}_{K_X}^*$, $E_{K_X}^*$ are the momenta and energies of the photon and the K_X system, respectively, calculated in the CM frame. In order to improve the M_{bc} resolution, the photon momentum is rescaled so that $|\vec{p}_\gamma^*| = (E_{beam}^* - E_{K_X}^*)/c$ is satisfied.

The largest source of background originates from continuum $q\bar{q}$ ($q = u, d, s, c$) production. To suppress this background, we use a Fisher discriminant [9] formed from six modified Fox-Wolfram moments [10] and the cosine of the B meson flight direction ($\cos\theta_B^*$). The moments are calculated in the rest frame of the B candidate to avoid a correlation with M_{bc} [11]. Signal and background events are classified according to a likelihood ratio $LR = \mathcal{L}_{sig}/(\mathcal{L}_{sig} + \mathcal{L}_{bg})$, where the likelihood \mathcal{L}_{sig} (\mathcal{L}_{bg}) is the product of the probability density functions (PDF) of the Fisher discriminant and $\cos\theta_B^*$ for signal (background). The PDFs for the Fisher discriminant are determined from Monte Carlo (MC) simulations. For $\cos\theta_B^*$, we assume a $1 - \cos^2\theta_B^*$ behavior for signal events and a flat distribution for continuum background. The selection criteria on the likelihood ratio are chosen so that $S/\sqrt{S+N}$ is maximized, where S and N are (MC) signal and background yields, respectively. The optimized criteria retain 68% of the $B^0 \rightarrow K^+\pi^-\gamma$ signal and 42% of the $B^+ \rightarrow K^+\pi^-\pi^+\gamma$ signal.

The B decay signal is separated from background, first by applying a requirement on ΔE and then by fitting the M_{bc} spectrum. If we find multiple candidates with $|\Delta E| < 0.5$ GeV and $M_{bc} > 5.2$ GeV/ c^2 in the same event, we take the candidate which gives the highest confidence level when we fit the K_X decay vertex (best candidate selection). We then select candidates with -100 MeV $< \Delta E < 75$ MeV, which removes 19% and 3% of signal on the lower and higher sides, respectively. We define a ΔE sideband to be 100 MeV $< \Delta E < 500$ MeV at $M_{bc} > 5.2$ GeV/ c^2 , in which we expect negligible signal contribution.

In the $B^0 \rightarrow K^+\pi^-\gamma$ analysis, we obtain the $M_{K\pi}$ distribution shown in Fig. 1(a). We observe an excess

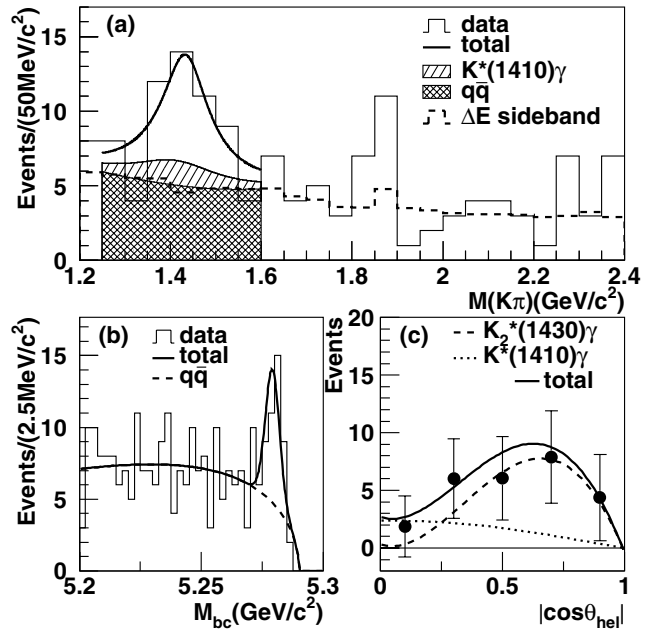


FIG. 1. (a) $M_{K\pi}$, (b) M_{bc} , and (c) $|\cos\theta_{hel}|$ distributions for $B^0 \rightarrow K^+\pi^-\gamma$ candidates. The unbinned ML fit results are shown in (a) and (c). The $q\bar{q}$ backgrounds are subtracted in (c). $M_{bc} > 5.27$ GeV/ c^2 is applied in (a) and (c), and 1.25 GeV/ $c^2 < M_{K\pi} < 1.6$ GeV/ c^2 is applied in (b) and (c). In (a), ΔE sideband data are scaled to the unbinned ML fit result and overlaid.

around $M_{K\pi} = 1.4$ GeV/ c^2 [12]. The M_{bc} distribution with 1.25 GeV/ $c^2 < M_{K\pi} < 1.6$ GeV/ c^2 is shown in Fig. 1(b). We fit the M_{bc} distribution to extract the signal yield. The distribution for the $q\bar{q}$ background is modeled by an ARGUS function [13] in which the shape is determined from the ΔE data sideband. The distribution for the signal component is modeled by a Gaussian determined from signal MC calibrated by $B^- \rightarrow D^0\pi^-$ data. The signal yield is found to be 27^{+8}_{-7} (stat) $^{+3}_{-3}$ (syst) with a statistical significance of 5.0σ . Here the significance is defined as $\sqrt{-2 \ln[\mathcal{L}(0)/\mathcal{L}_{max}]}$, where \mathcal{L}_{max} is the maximum of the likelihood and $\mathcal{L}(0)$ is the likelihood for zero signal yield.

The observed signal may be explained as a mixture of three components: $B^0 \rightarrow K_2^*(1430)^0\gamma$, $B^0 \rightarrow K^*(1410)^0\gamma$, and nonresonant (NR) $B^0 \rightarrow K^+\pi^-\gamma$. In order to separate these components, we apply an unbinned maximum likelihood (ML) fit to M_{bc} , the cosine of the decay helicity angle ($\cos\theta_{hel}$), and $M_{K\pi}$. The expected $\cos\theta_{hel}$ distributions are $\sin^2 2\theta_{hel}$, $\sin^2\theta_{hel}$, and uniform for these three components, respectively. The PDFs for $\cos\theta_{hel}$ and $M_{K\pi}$ are determined from the ΔE sideband data for $q\bar{q}$ background, from the corresponding MC samples for resonant components, and from an inclusive $b \rightarrow s\gamma$ MC sample [11] for the nonresonant component. The $\cos\theta_{hel}$ PDFs for signals are distorted up to 20% due to a nonuniform efficiency. The validity of the method is tested with $B^- \rightarrow D^0\pi^-$ data and MC.

The fit results for $M_{K\pi}$ and $\cos\theta_{\text{hel}}$ are overlaid in Figs. 1(a) and 1(c), and summarized in Table I. We find evidence for radiative decays via an intermediate tensor state, $B^0 \rightarrow K_2^*(1430)^0 \gamma$. The $K^*(1410)^0 \gamma$ and nonresonant components are not significant, so we set upper limits. The 90% confidence level upper limit N is calculated from the relation $\int_0^N \mathcal{L}(n) dn = 0.9 \int_0^\infty \mathcal{L}(n) dn$, where $\mathcal{L}(n)$ is the maximum likelihood with the signal yield fixed at n .

We estimate the systematic error due to the fitting procedure as follows. For the signal shapes in the M_{bc} and $M_{K\pi}$ distributions, we vary the mean and width parameters in the fit within their experimental errors. We also test the validity of the background PDFs by replacing them with those obtained from a $q\bar{q}$ MC sample. We assign the largest deviation in these tests as the systematic error of the signal yield.

The event selection efficiency for $B^0 \rightarrow K_2^*(1430)^0 \gamma$ is $(5.0 \pm 0.3)\%$ including the subdecay branching fractions. The error includes contributions from photon detection (2.8%), tracking (2.3% per track), kaon identification (0.6%), pion identification (0.5%), event selection including likelihood ratio, π^0/η veto and best candidate selection (2.0%), and uncertainty of the subdecay branching fractions (2.4%). Assuming an equal production rate for $B^0 \bar{B}^0$ and $B^+ B^-$, this leads to a branching fraction of $B^0 \rightarrow K_2^*(1430)^0 \gamma$ of $[1.3 \pm 0.5(\text{stat}) \pm 0.1(\text{syst})] \times 10^{-5}$.

The result agrees with the predictions based on a relativistic form factor calculation [4]. Our result is also consistent with the CLEO measurement [3] when we neglect the nonresonant component and assume as they did that the $K^*(1410)\gamma$ component is negligible.

In the $B^+ \rightarrow K^+ \pi^- \pi^+ \gamma$ analysis, we find additional background sources from a MC study. Cross feed from

$B \rightarrow K^* \gamma$ to $B^+ \rightarrow K^+ \pi^- \pi^+ \gamma$ becomes negligible after removing positively identified $B \rightarrow K\pi\gamma$ events. The size of the cross feed from other $b \rightarrow s\gamma$ decays, especially from those with a π^0 in the final state, is estimated by using the inclusive $b \rightarrow s\gamma$ MC sample. The contribution from the $b \rightarrow c$ background is estimated by using a corresponding MC sample.

To extract the signal yield, we fit the M_{bc} distribution shown in Fig. 2(a). In addition to a Gaussian and an ARGUS function to describe the signal and $q\bar{q}$ background components obtained using the same method as in the $B \rightarrow K\pi\gamma$ analysis, smoothed MC histograms for the $b \rightarrow s\gamma$ cross feed and other B meson decays are used to model the M_{bc} shape, where the normalizations are fixed assuming the luminosity and the measured $b \rightarrow s\gamma$ branching fraction [11,15]. We find the signal yield of $57_{-11}^{+12}(\text{stat})_{-2}^{+6}(\text{syst})$ with a 5.9σ statistical significance.

The $M_{K\pi}$ distribution is shown in Fig. 2(b), where the distribution for $q\bar{q}$ is obtained from the ΔE sideband and is normalized using the fit result. We observe no signal excess above $1.8 \text{ GeV}/c^2$. The $B^+ \rightarrow K^+ \pi^- \pi^+ \gamma$ signal may be explained as a sum of decays through kaonic resonances such as $B^+ \rightarrow K_1(1400)^+ \gamma$ and $B^+ \rightarrow K^*(1680)^+ \gamma$. The current statistics and the existence of a large number of resonances prevent us from decomposing the resonant substructure. However, it is still possible to measure the $K^* \pi\gamma$ and $K\rho\gamma$ components separately, as most of the resonances have sizable decay rates through the $K^* \pi$ and $K\rho$ channels.

To find the composition of the signal, we perform an unbinned ML fit to M_{bc} , $M_{K\pi}$, and $M_{\pi\pi}$ with three signal components ($K^* \pi\gamma$, $K\rho\gamma$, and nonresonant $K\pi\pi\gamma$) and a $q\bar{q}$ background component. In addition, the components from $b \rightarrow s\gamma$ cross feed and from other B meson decays

TABLE I. Measured signal yields, statistical significances, reconstruction efficiencies, branching fractions (\mathcal{B}), and 90% confidence level upper limits (UL) including systematic errors. The first and second errors are statistical and systematic, respectively. Efficiencies include the subdecay branching fractions [14]. Efficiencies for $K^+ \pi^- \gamma$ and $K^+ \pi^- \pi^+ \gamma$ are based on a mixture of the measured subcomponents.

Mode	Signal yield	UL (yield)	Significance	Efficiency(%)	$\mathcal{B} (\times 10^{-5})$	UL ($\times 10^{-5}$)
$K^+ \pi^- \gamma^a$	$27_{-7}^{+8}{}_{-3}^{+1}$...	5.0^c	18 ± 2	$0.46_{-0.12}^{+0.13}{}_{-0.07}^{+0.05}$...
$K_2^*(1430)^0 \gamma$	$21_{-7}^{+8}{}_{-1}^{+0}$...	3.2	5.0 ± 0.3	$1.3 \pm 0.5 \pm 0.1$...
$K^*(1410)^0 \gamma$	$7.7_{-5.7}^{+7.1}{}_{-1.3}^{+0.5}$	19	...	0.58 ± 0.12	...	13
$K^+ \pi^- \gamma$ (NR) ^a	$0.0_{-0.0}^{+4.6} \pm 0.0$	15	...	19 ± 1	...	0.26
$K^+ \pi^- \pi^+ \gamma^b$	$57_{-11}^{+12}{}_{-2}^{+6}$...	5.9^c	7.5 ± 0.7	$2.4 \pm 0.5_{-0.2}^{+0.4}$...
$K^{*0} \pi^+ \gamma^b$	$33_{-10}^{+11} \pm 2$...	3.7	5.0 ± 0.5	$2.0_{-0.6}^{+0.7} \pm 0.2$...
$K^+ \rho^0 \gamma^b$	$24 \pm 12_{-4}^{+4}$	43	2.2	7.4 ± 0.7	$1.0 \pm 0.5_{-0.3}^{+0.2}$	2.0
$K^+ \pi^- \pi^+ \gamma$ (NR) ^b	$0_{-0}^{+11} \pm 0$	20	...	7.6 ± 0.7	...	0.92
$K_1(1270)^+ \gamma$	$4.0 \pm 2.4 \pm 0.6$	10	...	0.40 ± 0.08	...	9.9
$K_1(1400)^+ \gamma$	$26 \pm 6_{-0}^{+2}$	36	...	2.6 ± 0.3	...	5.0

^a $1.25 \text{ GeV}/c^2 < M_{K\pi} < 1.6 \text{ GeV}/c^2$.

^b $M_{K\pi\pi} < 2.4 \text{ GeV}/c^2$.

^c M_{bc} fit result.

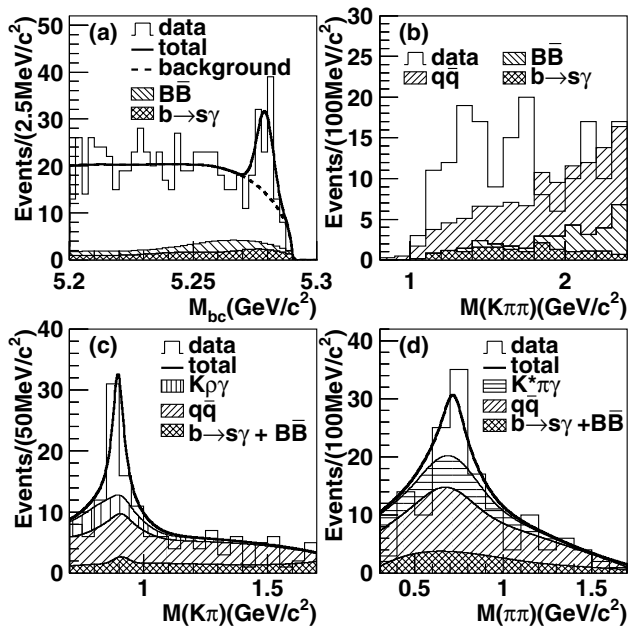


FIG. 2. (a) M_{bc} , (b) M_{K_X} , (c) $M_{K\pi}$, and (d) $M_{\pi\pi}$ distributions. The fit result of the M_{bc} distribution is shown in (a), while the result of the unbinned ML fit is shown in (c) and (d). $M_{bc} > 5.27 \text{ GeV}/c^2$ is applied in (b), (c) and (d).

are included in the fit with fixed normalizations. The $M_{K\pi}$ and $M_{\pi\pi}$ shapes for the $q\bar{q}$ background are determined from the ΔE sideband data, and those for the other components are determined from the corresponding MC samples.

In order to model the signal PDF for the $K^*\pi\gamma$ component, we use a mixture of $B^+ \rightarrow K_1(1400)^+\gamma \rightarrow K^{*0}\pi^+\gamma$ and $B^+ \rightarrow K^*(1680)^+\gamma \rightarrow K^{*0}\pi^+\gamma$ MC. The $K_1(1400)\gamma$ fraction of the mixture is determined to be 0.74 ± 0.14 by examining a background-subtracted $M_{K\pi\pi}$ distribution for candidates with $|M_{K\pi} - M_{K^*}| < 75 \text{ MeV}/c^2$ (K^* mass cut). Likewise for the $K\rho\gamma$ PDF, a mixture of $B^+ \rightarrow K_1(1270)^+\gamma \rightarrow K^+\rho^0\gamma$ and $B^+ \rightarrow K^*(1680)^+\gamma \rightarrow K^+\rho^0\gamma$ MC is used, where the $K_1(1270)\gamma$ fraction is determined to be 0.68 ± 0.17 according to a background-subtracted $M_{K\pi\pi}$ distribution for candidates with $|M_{\pi\pi} - M_\rho| < 250 \text{ MeV}/c^2$ and $|M_{K\pi} - M_{K^*}| > 125 \text{ MeV}/c^2$ (ρ mass cut).

Figures 2(c) and 2(d) show the distributions and fit results for $M_{K\pi}$ and $M_{\pi\pi}$. The selection efficiency is estimated from a MC sample with the mixture of resonances used for the PDF determination. We also consider other well-established resonances [16] which give slightly different efficiencies, and assign the difference in the result as a systematic error. The signal yields, the efficiencies, and the branching fractions are listed in Table I. The total $B^+ \rightarrow K^+\pi^-\pi^+\gamma$ branching fraction is dominated by $B^+ \rightarrow K^{*0}\pi^+\gamma$ and $B^+ \rightarrow K^+\rho^0\gamma$; the statistical significance for the sum of the two is calculated to be 6.2σ , and the nonresonant component is consistent with zero.

TABLE II. Exclusive and inclusive branching fractions for the $b \rightarrow s\gamma$ process. Equal branching fractions are assumed for neutral and charged B decays. Using isospin, the branching fraction of $B^+ \rightarrow K^{*+}\pi^0\gamma$ ($K^0\rho^+\gamma$) is assumed to be half (twice) that of $B^+ \rightarrow K^{*0}\pi^+\gamma$ ($K^+\rho^0\gamma$).

Mode	$\mathcal{B} (\times 10^{-5})$	Ref.
$B \rightarrow K^*\gamma$	4.2 ± 0.4	[3,17]
$B \rightarrow K_2^*(1430)\gamma$ (excluding $K^*\pi\gamma, K\rho\gamma$)	0.9 ± 0.3	
$B \rightarrow K^*\pi\gamma$	3.1 ± 1.0	
$B \rightarrow K\rho\gamma$	3.0 ± 1.6	
Sum of exclusive modes	11.2 ± 2.1	
$B \rightarrow X_s\gamma$ (inclusive)	32.2 ± 4.0	[11,15]

We find evidence for the decay $B^+ \rightarrow K^{*0}\pi^+\gamma$ with a 3.7σ significance, while the $B^+ \rightarrow K^+\rho^0\gamma$ channel alone yields only 2.2σ . Systematic errors are evaluated using the same procedures as in the $B \rightarrow K\pi\gamma$ analysis.

We also search for resonant decays by applying further kinematical requirements. We search for $B^+ \rightarrow K_1(1270)^+\gamma$ in the $K^+\rho^0\gamma$ final state by applying the ρ mass cut and $|M_{K_X} - M_{K_1(1270)}| < 100 \text{ MeV}/c^2$. We find six candidates with a background expectation of 2.0 ± 0.6 events. To find $B^+ \rightarrow K_1(1400)^+\gamma$ in the $K^{*0}\pi^+\gamma$ final state, we apply the K^* mass cut and $|M_{K_X} - M_{K_1(1400)}| < 200 \text{ MeV}/c^2$. We obtain a sizable signal; however, we provide only upper limits due to a lack of ability to distinguish these resonances. The results are also listed in Table I.

In conclusion, we have studied radiative B decays with the $K^+\pi^-\gamma$ and $K^+\pi^-\pi^+\gamma$ final states. For $K^+\pi^-\gamma$, we consider $B^0 \rightarrow K_2^*(1430)^0\gamma$, $B^0 \rightarrow K^*(1410)^0\gamma$, and non-resonant components, and find that only the first one is significant. For $B^+ \rightarrow K^+\pi^-\pi^+\gamma$, we observe the decay mode and measure the branching fraction. The branching fractions for $B \rightarrow K^*\pi\gamma$ and $K\rho\gamma$ are consistent with the sum of predicted rates of resonant decays [4]. As listed in Table II, we find $(35 \pm 8)\%$ of the total $B \rightarrow X_s\gamma$ decay is accounted for by the $B \rightarrow K^*\gamma$, $B \rightarrow K_2^*(1430)\gamma$, and $B \rightarrow K\pi\pi\gamma$ final states.

We thank the KEKB accelerator group for the excellent operation of the KEKB accelerator. We acknowledge support from the Ministry of Education, Culture, Sports, Science, and Technology of Japan and the Japan Society for the Promotion of Science; the Australian Research Council and the Australian Department of Industry, Science and Resources; the National Science Foundation of China under Contract No. 10175071; the Department of Science and Technology of India; the BK21 program of the Ministry of Education of Korea and the CHEP SRC program of the Korea Science and Engineering Foundation; the Polish State Committee for Scientific Research under Contract No. 2P03B 17017; the Ministry of Science and Technology of the Russian Federation; the Ministry of Education, Science and Sport of the

Republic of Slovenia; the National Science Council and the Ministry of Education of Taiwan; and the U.S. Department of Energy.

*On leave from Nova Gorica Polytechnic, Slovenia.

- [1] CLEO Collaboration, M. S. Alam *et al.*, Phys. Rev. Lett. **74**, 2885 (1995).
- [2] Hereafter, $K^*(892)$ is denoted by K^* .
- [3] CLEO Collaboration, T. E. Coan *et al.*, Phys. Rev. Lett. **84**, 5283 (2000).
- [4] S. Veseli and M. G. Olsson, Phys. Lett. B **367**, 309 (1996); D. Ebert *et al.*, Phys. Rev. D **64**, 054001 (2001); A. S. Safir, Eur. Phys. J. C **15**, 1 (2001).
- [5] M. Gronau *et al.*, Phys. Rev. Lett. **88**, 051802 (2002).
- [6] Belle Collaboration, A. Abashian *et al.*, Nucl. Instrum. Methods Phys. Res., Sect. A **479**, 117 (2002).
- [7] KEKB B Factory Design Report, KEK Report No. 95-1, 1995 (unpublished).
- [8] The charge conjugated modes are implicitly included.
- [9] R. A. Fisher, Annals Eugen. **7**, 179 (1936).
- [10] G. C. Fox and S. Wolfram, Phys. Rev. Lett. **41**, 1581 (1978).
- [11] Belle Collaboration, K. Abe *et al.*, Phys. Lett. B **511**, 151 (2001).
- [12] We expect $3 \pm 1 \bar{B}^0 \rightarrow D^0 \pi^0$ background which may account for the excess around $M_{K\pi} = 1.85 \text{ GeV}/c^2$.
- [13] ARGUS Collaboration, H. Albrecht *et al.*, Phys. Lett. B **229**, 304 (1989).
- [14] Particle Data Group, D. E. Groom *et al.*, Eur. Phys. J. C **15**, 1 (2000).
- [15] CLEO Collaboration, S. Chen *et al.*, Phys. Rev. Lett. **87**, 251807 (2001); ALEPH Collaboration, R. Barate *et al.*, Phys. Lett. B **429**, 169 (1998).
- [16] We consider $K_1(1270)$, $K_1(1400)$, $K^*(1410)$, $K_2^*(1430)$, $K_1(1650)$, and $K^*(1680)$.
- [17] BABAR Collaboration, B. Aubert *et al.*, Phys. Rev. Lett. **88**, 101805 (2002); Belle Collaboration, Y. Ushiroda *et al.*, hep-ex/0104045.